J. Appl. Comput. Mech., 3(4) (2017) 240-250
DOI: 10.22055/JACM.2017.21451.1099

ISSN: 2383-4536
jacm.scu.ac.ir

Shahid Chamran University of Ahvaz

Journal of Applied and Computational Mechanics

Research Article

Effect of variable thermal expansion coefficient and nanofluid properties on steady natural convection in an enclosure

Esmaeil Ghahremani[1], Reihaneh Ghaffari[1], Hossein Ghadjari[1], Javad Mokhtari[2]

[1] Department of Energy Engineering and Physics, Amirkabir University of Technology (Tehran Polytechnic), Tehran, Islamic Republic of Iran
[2] Department of Mathematics, Isfahan (Khorasgan) Branch, Islamic Azad University, Isfahan, Iran

Received March 07 2017; Revised April 29 2017; Accepted for publication May 03 2017.
Corresponding author: Esmaeil Ghahremani, eghahremani86@gmail.com

Abstract. Steady state natural convection is numerically investigated in an enclosure using variable thermal conductivity, viscosity and thermal expansion coefficient of Al_2O_3–water nanofluid. This study has been conducted for a wide range of Rayleigh numbers ($10^3 \leq Ra \leq 10^6$), concentrations of nanoparticles ($0\% \leq \Phi \leq 7\%$), enclosure aspect ratios ($0.5 \leq AR \leq 2$) and temperature differences between the cold and the hot walls ($1 \leq \Delta T \leq 30$). The main idea in this study is about the effect of temperature on natural convection pattern of nanofluid by changing nanoparticles concentration. Also, changing thermal expansion coefficient with temperature is considerd in this study which will have significant effects on natural convection and has not been considerd before. In low Rayleigh numbers ($Ra = 10^3$) and for cavities with $AR \geq 1$, the pattern shown in the average Nusselt number versus volume fraction of nanoparticles diagram deteriorates by increasing ΔT. However, for other cases, increasing ΔT has a positive effect on Nu-Φ diagram. The actual Nuselt number curve depicts that dispersing nanoparticles in base fluid deteriorate natural convection heat transfer which is in a good agreement with experimental works.

Keywords: Nanofluid; Natural convection; Variable property.

1. Introduction

Natural convection in enclosure is an important phenomenon and has extensively attracted attention because of its wide applications in electronics cooling, solar collectors, heat exchangers and so on [1-3]. Using dispersed nano-scale particles especially metallic or metallic oxide in base fluid, known as nanofluid [4] is a technique for improving the heat transfer coefficient of the base fluid. However, there are contradictory remarks about natural convection of nanofluid.

In many numerical studies [5-7] the effective viscosity of nanofluid is accounted by Brinkman model [8] and these studies have showed that the average Nusselt number for the nanofluids is more than that of the base fluids. Polidori et al. [9] and Ho et al. [10] used Maiga model [11] to express the viscosity of nanofluids. Their results indicated a slight reduction of heat transfer rate for nanofluid by increasing nanoparticles volume fraction. Aminossadati and Ghasemi [12] investigated the natural convection of nanofluid by means of Brownian model [13, 14] to describe nanofluid properties. Their study showed that the average Nusselt number increases for nanofluid. The investigation of natural convection of nanofluids in enclosure cavity with variable properties was performed by Abu-Nada et al. [15]. They declared that when Ra=1000, the heat transfer rate improves by increasing nanoparticles concentration; but for Ra>1000, the mentioned parameter reduces by enhancing the nanoparticles volume fraction more than 1%.

Controversial debates also exist about experimental work on natural convection. Some experimental studies [16, 17] depicted an enhancement in the natural convection heat transfer by adding nanoparticles to the base fluid; however, some others [18-22] showed contradictory results. Some other experimental studies [23, 24] expressed that the effect of nanoparticles dispersion in base fluids on the natural convection heat transfer depends on solid volume fraction and Rayleigh number. Nnanna et al. [16] experimentally observed that adding Cu nanoparticles to ethylene glycol improves the natural convection heat transfer. Nnanna

Published Online: May 04 2017

and Routhu [17] experimentally achieved similar enhancement for Alumina–Water nanofluids. Putra et al. [18] carried out an experimental study to investigate the natural convection heat transfer of Al2O3 and CuO–water nanofluids inside a horizontal cylinder heated from one end and cooled from the other for Rayleigh numbers ranging from 106 and 109. Nanoparticles concentration and aspect ratio varied between 1% and 4% and 0.5 and 1.5, respectively. They found out that the natural convection heat transfer decreases systematically by adding nanoparticles to the base fluid; Deterioration escalates with increasing particles concentration particularly for CuO–water nanofluid. Wen and Ding, experimentally investigated the natural convection of water–TiO2 nanofluid in an enclosure [19] and a vessel composed of two discs [20] both heated from bellow. They reported that for the Rayleigh numbers less than 106, the natural convection heat transfer rate drastically decreased with the increase of particle concentration, particularly at low Rayleigh numbers. Moreover, an experimental study [21] on natural convection of Al2O3–water nanofluid in a vertical cylindrical enclosure heated from below with the nanoparticles volume concentration between 0.5% and 6%, showed that the heat transfer rate across the enclosure is deteriorated increasingly by the enhancement of solid volume fraction. More recently, experimental and numerical investigations on the natural convection heat transfer of TiO2–water nanofluids in a square enclosure were conducted by Hu et al. [22]. Experimental results show that the natural convection heat transfer of nanofluids is not better than water and even worse when the Rayleigh number is low. In a vertical long enclosure with an aspect ratio of 6.14, Nnanna [23] experimentally observed that the natural convection heat transfer increases for nanofluids of volume fractions ranging from 0.2% to 2% and decreases for nanofluids with volume fractions above 2%. Ho et al. [24] carried out an experimental study on the natural convection heat transfer of Al2O3–water nanofluids in three different sizes of square enclosures. For all ranges of Rayleigh Numbers, they observed a decrease for the nanofluid's Nusselt number with volume fractions above 2%. However, compared to water, for nanofluids containing much lower particle fraction for example, 0.1 vol%, a heat transfer enhancement of about 18% was found in the largest enclosure at sufficiently high Rayleigh numbers.

In previous numerical studies, various models are used for representing nanofluid properties and these models have got more precision over time. In general, adding a little amount of nanoparticles to base fluid leads to the increase of the average Nuselt number but average Nuselt number is deteriorated by increasing nanoparticles concentration. Although, experimental works have different results, in general, actual Nuselt number diminishes with increasing nanoparticle concentration.

The properties of nanofluids change with temperature and these changes are recently considered in numerical simulations. Water expansion coefficient also depends on temperature, and its value at 50 °C is twice as much more than the value at 20 °C. However, no numerical studies have inspected the natural convection with variable expansion coefficient. Similarly previous experimental works neglected the impact of average fluid temperature on natural convection heat transfer. Furthermore, transient natural convection solution as non-dimensional case hasn't been considered in any previous numerical studies for a better assessment. This study investigates the steady state natural convection of Al2O3–water nanofluid with variable properties and thermal expansion coefficient in a rectangular cavity.

2. Mathematical formulation

Fig.1 shows the schematic diagram of a two-dimensional square cavity that is filled with water-Al_2O_3 nanofluid. The height and the width of the cavity are noted by H and W respectively and aspect ratio (AR) is defined as W/H. Nanofluid is considered single phase and homogenous. Diameter of nanoparticles is considered to be equal to 47 nanometers. Table 1 presents the thermophysical properties of base fluid (water) and nanoparticles at T=20 °C. It is assumed that nanofluid flow is laminar and incompressible. Both viscosity and thermal conductivity of the nanofluid are considered variable.

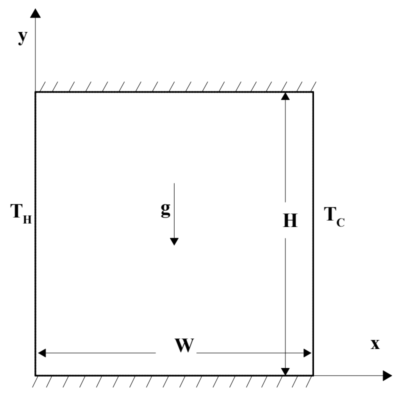

Fig.1. Schematic diagram of the physical model for the enclosure.

Table 1. Physical properties of pure water and Al_2O_3 nanoparticles

	ρ (kg m^{-3})	C_P (J kg^{-1}K^{-1})	k (Wm^{-1}K^{-1})	β (K^{-1})
Pure water	998.2	4179	0.603	2.064×10^{-4}
Al_2O_3	3970	765	25	8.5×10^{-6}

For the transient natural convection; continuity, momentum and energy equations in two-dimensional cavity can be written in non-dimensional forms as follows:

$$\frac{\partial U}{\partial X}+\frac{\partial V}{\partial Y}=0 \tag{1}$$

$$U\frac{\partial U}{\partial X}+V\frac{\partial U}{\partial Y}=-\frac{1}{\rho}\frac{\partial P}{\partial X}+\frac{\mu_{f_0}}{\rho_{nf}\alpha_{f_0}}\left(2\frac{\partial}{\partial X}\left(\mu\frac{\partial U}{\partial X}\right)+\frac{\partial}{\partial Y}\left(\mu\frac{\partial U}{\partial Y}\right)+\frac{\partial}{\partial Y}\left(\mu\frac{\partial V}{\partial X}\right)\right) \tag{2}$$

$$\begin{aligned}U\frac{\partial V}{\partial X}+V\frac{\partial V}{\partial Y}=&-\frac{1}{\rho}\frac{\partial P}{\partial Y}+\frac{\mu_{f_0}}{\rho_{nf}\alpha_{f_0}}\left(2\frac{\partial}{\partial Y}\left(\mu\frac{\partial V}{\partial Y}\right)+\frac{\partial}{\partial X}\left(\mu\frac{\partial V}{\partial X}\right)+\frac{\partial}{\partial X}\left(\mu\frac{\partial U}{\partial Y}\right)\right)\\&+\frac{\rho_{f_0}}{\rho_{nf}}\left((1-\varphi)f(\beta_T)+\varphi\frac{\rho_{np}\beta_{np}}{\rho_{f_0}\beta_{f_0}}\right)Ra\Pr\theta\end{aligned} \tag{3}$$

$$U\frac{\partial\theta}{\partial X}+V\frac{\partial\theta}{\partial Y}=\frac{\partial}{\partial X}\left(\alpha\frac{\partial\theta}{\partial X}\right)+\frac{\partial}{\partial Y}\left(\alpha\frac{\partial\theta}{\partial Y}\right) \tag{4}$$

In the above equations, the following non-dimensional parameters are used:

$$\begin{gathered}X=\frac{x}{H}\ ,\quad \mathrm{Y}=\frac{y}{H}\ ,\quad \mathrm{U}=\frac{\mathrm{uH}}{\alpha_{f_0}}\ ,\quad V=\frac{vH}{\alpha_{f_0}}\ ,\quad P=\frac{\bar{p}H^2}{\rho_{nf}\alpha_{f_0}^2}\\ \theta=\frac{T-T_c}{T_h-T_c}\ ,\quad Ra=\frac{g\beta_{f_0}H^3(T_h-T_c)}{\vartheta_{f_0}\alpha_{f_0}}\ ,\quad \Pr=\frac{\vartheta_{f_0}}{\alpha_{f_0}}\ ,\quad \mu=\frac{\mu_{nf}}{\mu_{f_0}}\ ,\quad \alpha=\frac{\alpha_{nf}}{\alpha_{f_0}}\end{gathered} \tag{5}$$

The actual Rayleigh number is also defined as:

$$Ra=\frac{g\beta H^3(T_h-T_c)}{\vartheta\alpha} \tag{6}$$

Where, fluid properties are calculated at average fluid temperature ($\frac{T_h+T_c}{2}$). The nanofluid density is written as:

$$\rho_{nf}=(1-\varphi)\rho_f+\varphi\rho_{np} \tag{7}$$

Also, the thermal diffusivity of nanofluid is expressed as:

$$\alpha_{nf}=k_{eff}\Big/(\rho C_p)_{nf} \tag{8}$$

And, the heat capacitance and the thermal expansion coefficient of nanofluid are equaled to:

$$(\rho C_p)_{nf}=(1-\varphi)(\rho C_p)_f+\varphi(\rho C_p)_{np} \tag{9}$$

$$(\rho\beta)_{nf}=(1-\varphi)(\rho\beta)_f+\varphi(\rho\beta)_{np} \tag{10}$$

The effective coefficient of thermal expansion of the nanofluid, β_{eff}, is defined by:

$$(\rho\beta)_{eff}=-\frac{d\rho_{eff}}{dT} \tag{11}$$

And thermal expansion coefficient of the base fluid for temperature range between 15 – 65 °C is considered with polynomial function as:

$$\beta_f(T)=10^{-4}\times(5.3546\times10^{-6}\mathrm{T}^3-1.2193\times10^{-3}\mathrm{T}^2+0.1469\mathrm{T}-0.4296) \tag{12}$$

Where, T is temperature in °C. With substituting Eqs. 10 and 12 in Eq. 11 and integrating it, temperature dependence of the expansion coefficient is defined as:

$$f(\beta_T)=\frac{\beta(T)}{\beta_{f_0}}=\left(\frac{1}{T-T_0}\int_{T_0}^{T}\beta_{\mathrm{f}}\,dT\right)\Big/\beta_{f_0} \tag{13}$$

and then:

$$f(\beta_T)=(\frac{1}{\beta_{f_0}})(1.3386\times10^{6}(T+T_0)(T^2+T_0^2)-4.0644\times10^{4}(T^2+TT_0+T_0^2)+0.0735(T+T_0)-0.4296) \tag{14}$$

Contours of f (β_T) pure water at Ra=10^5 is shown in Fig. 2. Temperature differences between cooled and heated walls (ΔT) are considered 1 and 30 °C. one can see from this figure that the buoyancy force changes with temperature and its value is increased by enhancing water temperature.

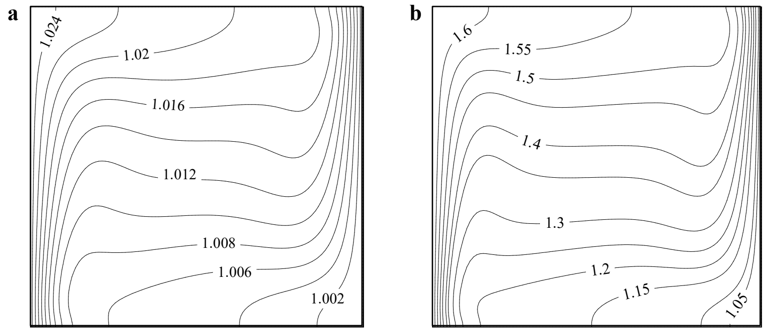

Fig. 2. Contours of $f(\beta_T)$, a) for ΔT=1 °C, b) for ΔT=30 °C.

Dimensionless effective dynamic viscosity (μ_{eff}/μ) is independent of temperature at least for temperatures which are not very different with room temperature and defined as [25]:

$$\frac{\mu_{eff}}{\mu_f}=\frac{1}{1-34.87(d_p/d_f)^{-0.3}\varphi^{1.03}} \tag{15}$$

The nanoparticles volume fraction and the nanofluid temperature lie in the ranges between 0.0001 and 0.071, and between 20 °C and 50 °C, respectively. According to [26], $\mu_f(T)$ can be calculated by:

$$\log\left(\frac{\mu_f(T)}{\mu_{f_0}}\right)=\frac{T_0-T}{T+96}\left[1.2378-1.303\times10^{-3}(T_0-T)+3.06\times10^{-6}(T_0-T)^2+2.55\times10^{-8}(T_0-T)^3\right] \tag{16}$$

That T_0 is 20 °C and this model considers temperature effect on base fluid with a wide range of temperature between -8 and 150 °C. Effective thermal conductivity of the nanofluid is determined from [25]:

$$\frac{k_{eff}}{k_f}=1+4.4\,\mathrm{Re}^{0.4}\,\mathrm{Pr}^{0.66}\left(\frac{T}{T_{fr}}\right)^{10}\left(\frac{k_s}{k_f}\right)^{0.03}\varphi^{0.66} \tag{17}$$

Where Pr is the Prandtl number of the base liquid, T is the nanofluid temperature in *K*, T_{fr} is the freezing point of the base liquid in K, k_s is the thermal conductivity of the solid nanoparticles, and φ is the nanoparticles volume fraction. *Re* is the nanoparticles Reynolds number:

$$\mathrm{Re}=\frac{2\rho_f k_b T}{\pi\mu_f^{\,2} d_p} \tag{18}$$

That k_b is the Boltzmann constant ($k_b=1.3807\times10^{-23}$ *J/K*). All of properties calculate at the nanofluid temperature – see [27] -. For the pure water, k_f is [27]:

$$k_f(T)=0.797015\,T^{*-0.194}-0.251242\,T^{*-4.717}+0.096437\,T^{*-6.385}-0.032696\,T^{*-2.134} \tag{19}$$

Where T^* is a dimensionless temperature given by $(T+273.15)/300$. The boundary conditions used to solve Eqs. (1) to (4) are as follows:

$$\begin{aligned}&\text{On the walls}:\ U=V=0\\&\text{On the horizontal adiabatic walls}:\ \frac{\partial\theta}{\partial Y}=0\\&\text{On the heated walls}:\ \theta=1\\&\text{On the cold walls}:\ \theta=0\end{aligned} \tag{20}$$

The local and the average Nusselt numbers for the vertical heated or cooled wall are given by:

$$Nu = -\frac{k_{eff}}{k_{f_0}}\left(\frac{\partial\theta}{\partial X}\right)_{on\ the\ \text{heated or cooled wall}} \tag{21}$$

$$\overline{Nu} = \int_{on\ the\ \text{heated or cooled wall}} Nu \quad dY \tag{22}$$

The local and the average actual Nusselt numbers for heated wall are also calculated as:

$$Nu_{act} = -\left(\frac{\partial\theta}{\partial X}\right)_{on\ the\ \text{heated wall}} \tag{23}$$

$$\overline{Nu_{act}} = \int_{on\ the\ \text{heated wall}} Nu_{act} dY \tag{24}$$

3. Numerical approach

The finite volume method [28, 29] is used to solve the governing Eqs. (1) – (4) with the corresponding boundary conditions given in Eq. (20). Both second-order implicit and explicit schemes are adopted to deal with the discretization of temporal terms in the governing equations. The SIMPLE algorithm is utilized to solve the coupling between velocity and pressure. Convection-diffusion terms are discretized by Hybrid scheme and the system is numerically modeled in FORTRAN. The solution procedure is iterated in every step until the two following convergence criterions are satisfied:

$$Max\left(\chi_{i,j}^{new} - \chi_{i,j}^{old}\right) \prec 10^{-7} \tag{25}$$

$$\sum_{i,j}\left(\frac{\chi_{i,j}^{new} - \chi_{i,j}^{old}}{\chi_{i,j}^{new}}\right) \prec 10^{-6} \tag{26}$$

Where, χ in Eqs. (25) and (26) is U, V, θ and the residual mass of the grid control volume. The numerical results of this work are compared with those of former studies in terms of natural convection in a cavity with vertical hot and cold walls in an air-filled enclosure with Pr=0.7 at different values of Rayleigh numbers as presented in Table 2. To ensure the grid independency of the numerical solutions, different grids have been tested for the case of water (Φ=0) at Ra=105 as listed in Table 3. To accomplish this, eight combinations of spatial resolution are considered. The relative deviations of the measure are also given with reference to that of the case with the finest spatial (120×120). The difference between the spatial 100×100 and 120×120 is negligible, so 100×100 grid is used in this study.

Table 2. Comparison of results for average Nusselt number in an air-filled square enclosure at different values of Rayleigh number and Pr=0.7.

Ra_f	Nu_m			
	present	Ho et al. [10]	Barakos Mitsoulis[3]	Fuseyi Hyun [30]
10^4	2.248	2.246	2.245	2.302
10^5	4.539	4.522	4.510	4.646
10^6	8.908	8.825	8.806	9.012

Table 3. Grid independency (Ra=105, Φ =0)

Number of cells	Nusselt number	Deviation (%)
60×60	6.0753	0.0162
80×80	6.0338	0.0091
100×100	5.9820	0.0004
120×120	-	-

4. Results and discussion

The ranges of the Rayleigh numbers value, volume fractions of nanoparticles, and the aspect ratios used in this work are Ra=103 -106, $0 \le \Phi \le 7$ %, and $0.5 \le AR \le 2$, respectively. The temperature of the enclosure's right wall is fixed at the reference temperature i.e., 20 °C, whereas the difference between the hot and the cold walls is varied between 1-30 °C. The Prandtl number at the reference temperature is calculated as 6.93.

Fig. 3 displays the local Nusselt numbers (Nu) distributions along the heated surface for various values of nanoparticles volume fractions (Φ = 0%, 1%, 4%, 7%) and Rayleigh numbers (Ra=103,104, 105, 106) for a square cavity (AR=1) when temperature differences between the cold and the hot walls are 1 and 30 °C. It is obvious that for all Rayleigh numbers, when ΔT is enhanced, the local Nusselt number increases along the hot wall due to the increase of the thermal expansion coefficient of the base fluid. The difference between Φ = 1% and the pure fluid case is negligible whereas the effect of nanoparticles on the local Nusselt number becomes more evident at higher concentrations. As the temperature difference between the cold and the hot walls increases, the locations wherein the addition of nanoparticles improves the local Nusselt number is shifted to the upper half of the heated surface particularly at low Rayleigh numbers (this location shifts from y≈0.5 for ΔT=1 toward y≈0.6 for ΔT=30 °C for the case of Ra=103).

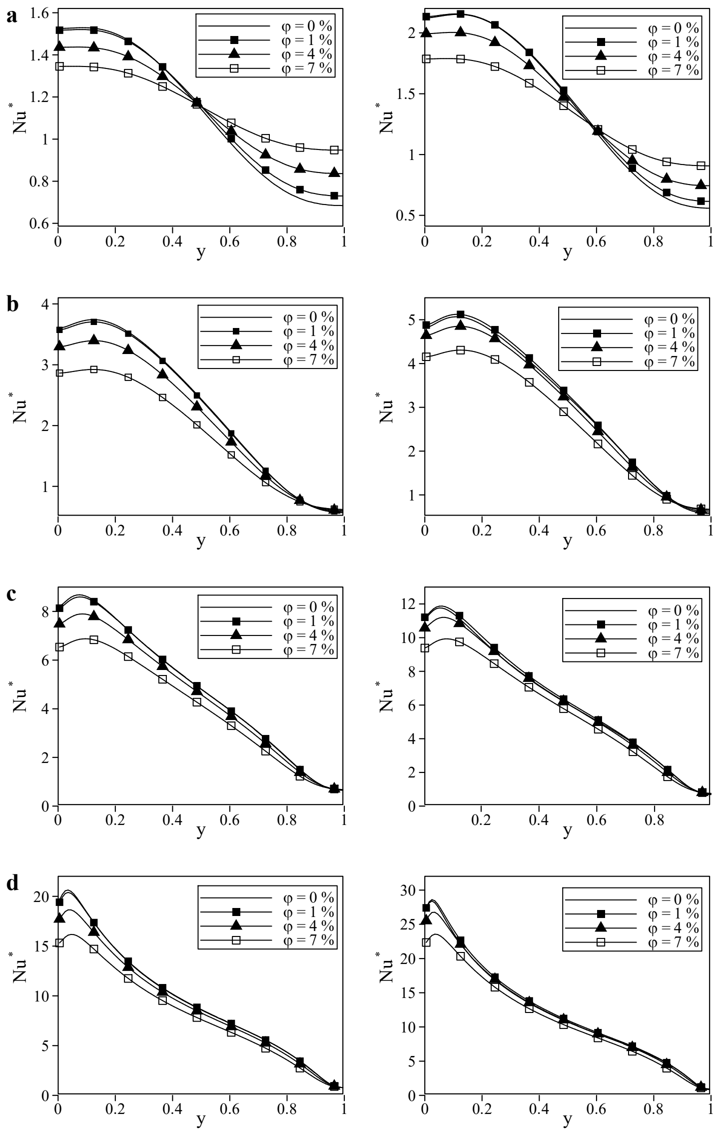

Fig. 3. Local Nusselt number for the case of ΔT=1 °C (left column) and ΔT=30 °C (right column), a) Ra=10^3, b) Ra=10^4, c) Ra=10^5, d) Ra=10^6.

The contour maps regarding the streamlines of Al2O3-Water nanofluid filled in a square cavity at Ra=103-106, are plotted in Fig. 4 for different values of the nanoparticles volume fraction (Φ = 0%, 1%, 4%, 7%) and ΔT=30 °C. As Φ increases, the streamline contours show deterioration in the absolute values of the maximum stream functions at Ra=103. For the case of nanofluid with Φ = 7%, the absolute maximum stream function is 47% less than that of pure water. At other Rayleigh numbers, higher absolute value of the maximum stream functions corresponds to the nanofluid with 1% nanoparticles volume fraction. At Ra=105 and Ra=106, the maximum values of the absolute stream function for the nanofluid with 4% nanoparticles concentrations are more than that of pure water which are still lower than the values for the nanofluid with a volume fraction of 1%. The absolute vertical velocity component at the enclosure mid-section is decreased with enhancement of φ due to the increase of the fluid viscosity; however, as shown in Fig. 5, heat diffuses more through the cavity because the thermal conductivity coefficient increases. It is also seen from Fig. 5 that the vertical velocity is asymmetric, i.e. its value is higher in the left hand side of the cavity around the heated surface and that is because the fluid's thermal expansion coefficient at the left section of the cavity is higher than the other side (Fig. 2).

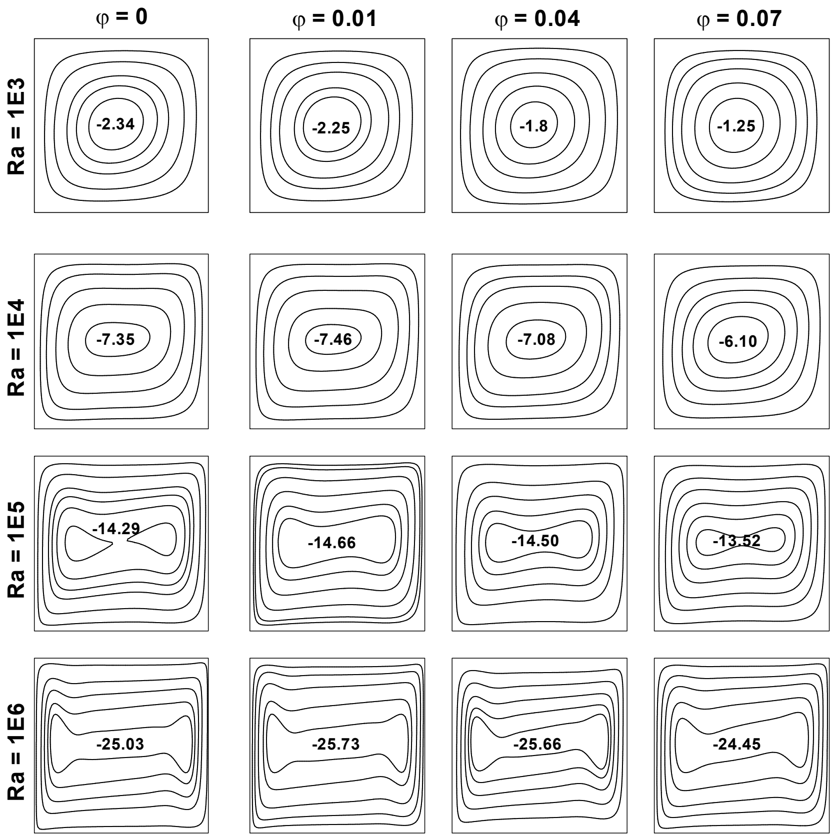

Fig. 4. Contours of streamlines in square enclosure for ΔT=30 °C.

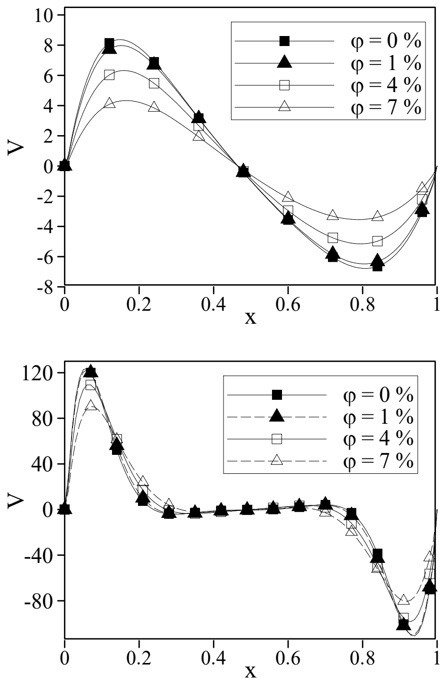

Fig. 5. Vertical velocity component at the enclosure mid-section, a) Ra=10^3, b) Ra=10^5.

Fig. 6 shows the average Nusselt number and the normalized average Nusselt number for a wide range of the cold and the hot walls temperature differences (ΔT) for the case of AR=1. Average Nusselt number slightly increases at low ΔTs when the volume fraction of nanoparticles is increased from zero (clear fluid) to 7% for the case of Ra = 103. However, the addition of nanoparticles to the base fluid causes the average Nusselt number to deteriorate for higher ΔTs in comparison with lower ΔTs. For low Rayleigh numbers (Ra=103) and low ΔTs, heat transfer is dominated by conduction and hence thermal conductivity determines the heat transfer rate. By rising ΔT, convection becomes the principal phenomenon in the heat transfer rate and viscosity effect dominates the favorable thermal conductivity effects when solid volume fraction increases. As φ increases, the average Nusselt number is diminished for the case of Ra=104 - 106 at law ΔT. This trend of decreasing is mitigated as the temperature difference between the cold and the hot walls is intensified. When ΔT is assumed 30, the average Nusselt number for the nanofluid with Φ = 1% and Φ = 2% is more than that of pure water. It is also evident from this figure that for all ranges of ΔT, deterioration is more significant for the case of Ra=104 with dispersion of nanoparticles in the base fluid, because inertia forces are smaller compared to those of Ra=105 and 106 as mentioned in [31].

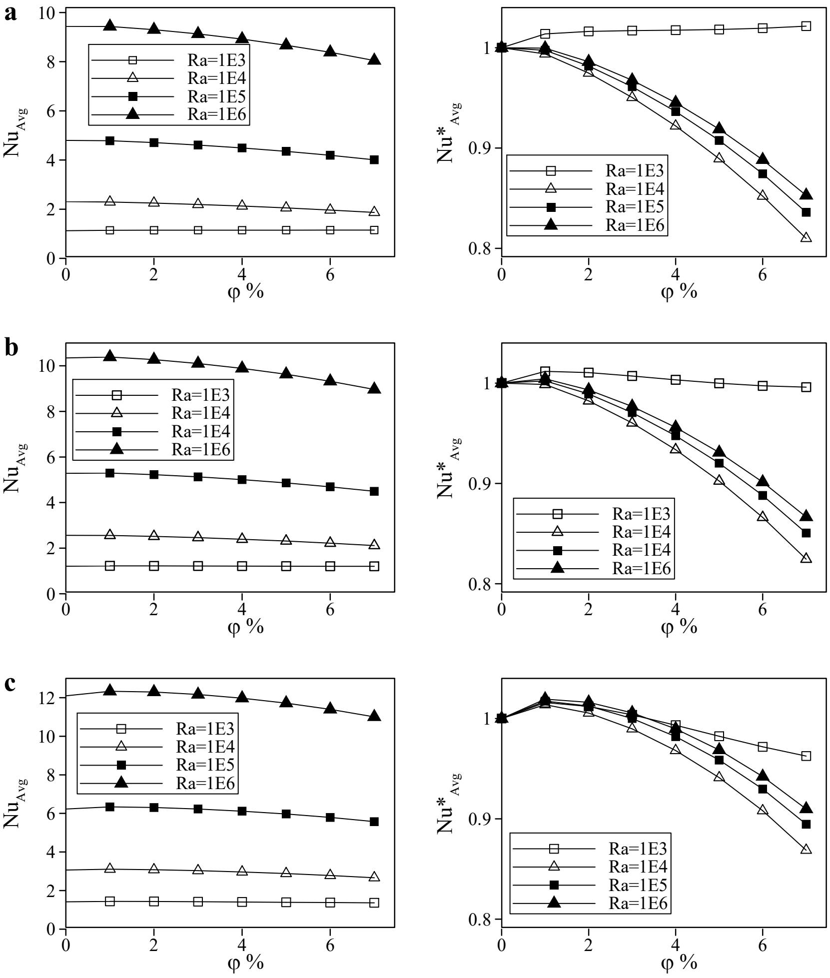

Fig. 6. Average Nusselt number (left column) and normalized average Nusselt number (right column) for square enclosure, a) ΔT=1 °C, b) ΔT=10 °C and c) ΔT=30 °C.

Fig. 7 displays the normalized average Nusselt number along the heated wall with a variety of nanoparticles volume fractions for the nanofluid, the Rayleigh numbers and ΔTs for the cavity with different aspect ratios. In a cavity with AR=0.5, adding nanoparticles to the pure water has a positive effect on the average Nusselt number at Ra=103 and its effect becomes more significant by increasing ΔT due to the domination of conduction [32]. Heat conduction coefficient of the nanofluid will increase by augmenting the fluid temperature. This behavior contradicts with that of the cavities with AR=1 and AR=2. For Ra=103, rising nanoparticles concentration leads to reduction of the average Nusselt number for a cavity with AR= 2 and its negative effect becomes more noticeable as ΔT increases. For AR=2, heat transfer is accomplished by conduction and convection at low ΔT, but convective heat transfer becomes dominant by enhancing ΔT. For the case of Ra=104, increasing the nanoparticles concentration has the worst effect on the average Nusselt number for AR=2, but for AR=0.5 and at lower ΔTs, its negative effect is less than that the cases of Ra=105 and Ra=106. In general, the average Nusselt number is less sensitive to aspect ratio for Ra=105 and Ra=106.

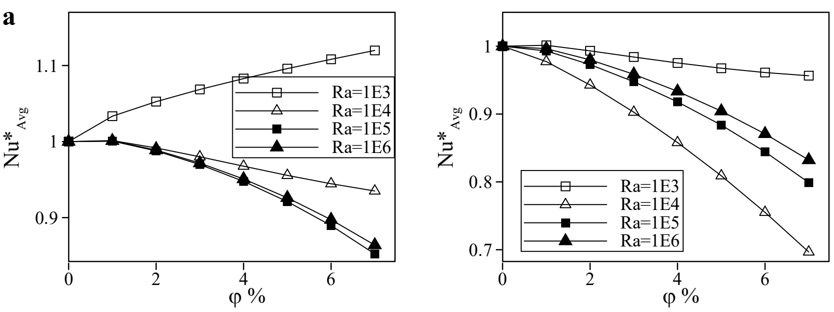

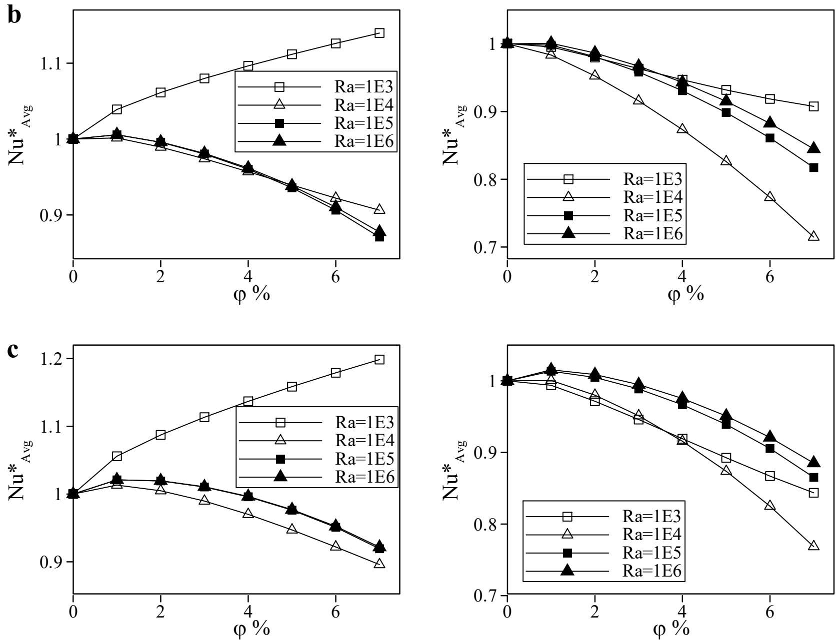

Fig. 7. Normalized average Nusselt number for the enclosure with AR=0.5 (left column) and AR=2 (right column), a) ΔT=1 °C, b) ΔT=10 °C and c) ΔT=30 °C.

Fig. 8 depicts the average actual Nusselt number – as defined by correlation (24) – versus actual Rayleigh number for ΔT=30 °C. A generic correlation equation in the form of power function with a coefficient of determination of R^2=0.9982 is presented here, that is valid for Rayleigh numbers in the range of 10^3-10^6.

$$\overline{Nu}_{act} = 0.0589 Ra_{act}^{\ 0.3103} \tag{27}$$

From Fig. 9 it is realized that pure water is the only fluid which is located above the curve for Ra≥104. Addition of nanoparticles to the base fluid deteriorates both the actual Nusselt number and the actual Rayleigh number. It is worth to mention this deterioration escalates with decreasing temperature differences between cooled and heated walls (decreasing in average fluid temperature).

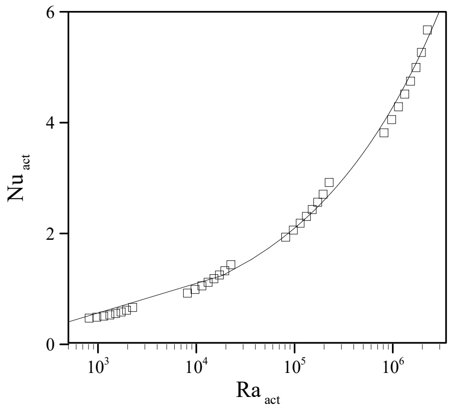

Fig.8. Actual average Nusselt number

5. Conclusion

Steady state natural convection heat transfer of Al2O3-water nanofluid in an enclosure with vertical hot and cold walls is investigated numerically. Considering the impact of fluid temperature on thermal expansion coefficient causes totally different patterns in natural convection heat transfer by increasing nanoparticle concentration. For all ranges of Rayleigh numbers, heat transfer intensifies by increasing the temperature difference between the cold and the hot walls (i.e. increasing the average temperature of the fluid) due to the enhancement of the thermal expansion coefficient. For all cases except AR ≥ 1 at Ra = 103, a reduction in the temperature difference of the cold and the hot walls, deteriorates the relation between the average Nusselt number and the nanoparticles volume fraction. In general, the average actual Nusselt number decreases with nanoparticles concentration increment.

Nomenclature

Cp	specific heat, J/(kgK)
d_f	molecule water diameter
d_p	nanoparticles diameter
g	gravitational acceleration, m/s^2
k	thermal conductivity, W/(mK)
k_b	Boltzmann constant
L	length of the cavity, m
Nu	local Nusselt number on the heated or cooled wall
$\overline{Nu}$	average Nusselt number
p	fluid pressure, Pa
$\overline{p}$	modified pressure
P	dimensionless pressure
Pr	Prandtl number
R_{np}	radius of nanoparticles, m
Ra	Rayleigh number
T	temperature, K or °C
T_c	cooled wall temperature, K or °C
T_h	heated wall temperature, K or °C
T_{fr}	freezing point temperature, K
u, v	velocity components in x, y directions, m/s
U, V	dimensionless velocity components
x, y	Cartesian coordinates, m
X, Y	dimensionless coordinates

Greek symbols

α	thermal diffusivity, m^2/s
β	thermal expansion coefficient, 1/K
φ	solid volume fraction
μ	dynamic viscosity, Ns/m^2
ν	kinematic viscosity, m^2/s
θ	dimensionless temperature
ρ	density, kg/m^3

Subscripts

act	actual
eff	effective
f	fluid (pure)
nf	nanofluid
s	solid nanoparticle
np	nanoparticle
0	reference value at 20 °C

References

[1] Vahl Davis, G.D. Natural convection of air in a square cavity, a benchmark numerical solution, *Int. J. Numer. Methods Fluids*, 3, 1962, pp. 249–264.
[2] Fusegi, T., Hyun, J.M., Kuwahara, K. Farouk, B. A numerical study of three-dimensional natural convection in a differentially heated cubical enclosure, *Int. J. Heat Mass Transfer*, 34, 1991, pp. 1543–1557.
[3] Barakos, G. Mitsoulis, E. Natural convection flow in a square cavity revisited: laminar and turbulent models with wall functions, *Int. J. Numer. Methods Fluids*, 18, 1994, pp. 695–719.
[4] Choi, U.S. Enhancing thermal conductivity of fluids with nanoparticles, *ASME Fluids Engineering Division*, 231, 1995, pp. 99–103.
[5] Xuan, Y., Roetzel, W. Conceptions for heat transfer correlation of nanofluids, *Int. J. Heat Mass Transfer*, 43, 2000, pp.3701–3707.
[6] Khanafer, K., Vafai, K. Lightstone, M. Buoyancy-driven heat transfer enhancement in a two-dimensional enclosure utilizing nanofluids, *Int. J. Heat Mass Transfer*, 46, 2003, pp. 3639–3653.

[7] Gosselin, L. da Silva, A.K. Combined heat transfer and power dissipation optimization of nanofluid flows, *Appl. Phys. Lett.*, 85, 2004, pp.4160–4162.
[8] Brinkman, H.C. The viscosity of concentrated suspensions and solutions, *J. Chem. Phys.*, 20, 1952, pp.571–581.
[9] Polidori, G., Fohanno, S. Nguyen, C.T. A note on heat transfer modeling of Newtonian nanofluids in laminar free convection, *Int. J. Thermal Sciences*, 46, 2007, pp. 739–744.
[10] Ho, C.J., Chen, M.W. Li, Z. W. Numerical simulation of natural convection of nanofluid in a square enclosure: Effects due to uncertainties of viscosity and thermal conductivity, *Int. J. Heat and Mass Transfer*, 51, 2008, pp. 4506–4516.
[11] Maiga, S.E.B., Nguyen, C.T., Galanis, N., Roy, G. Heat transfer behaviors of nanofluids in a uniformly heated tube, *Superlattices and Microstructures*, 35, 2004, pp. 543–557.
[12] Aminossadati, S.M. Ghasemi, B. Natural convection of water–CuO nanofluid in a cavity with two pairs of heat source–sink, *Int. Comm. in Heat and Mass Transfer*, 38, 2011, pp. 672-678.
[13] Koo, J. Kleinstreuer, C. A new thermal conductivity model for nanofluids, *J. Nanoparticle Research*, 6(6), 2004, pp. 577–588.
[14] Koo, J. Kleinstreuer, C. Laminar nanofluid flow in micro heat-sinks, *Int. J. Heat and Mass Transfer*, 48(13), 2005, pp. 2652–2661.
[15] Abu-Nada, E., Masoud, Z., Oztop, H.F. Campo, A. Effect of nanofluid variable properties on natural convection in enclosures, *Int. J. Thermal Sciences*, 49, 2010, pp. 479–491.
[16] Nnanna, A.G.A., Fistrovich, T., Malinski, K. Choi, S.U.S. Thermal transport phenomena in buoyancy-driven nanofluids, *Proc. ASME Int. Mech. Eng. Congress RDD Expo., IMECE2004-62059*, Anaheim, CA, 2004, pp. 1-8.
[17] Nnanna, A.G.A. Routhu, M. Transport phenomena in buoyancy driven nanofluids Part II, *Proc. ASME Summer Heat Transfer Conf.*, SHTC— 72782, San Francisco, CA, 2005, pp. 1–8.
[18] Putra, N., Roetzel, W. Das, S.K. Natural convection of nanofluids, *Heat Mass Transfer*, 39, 2003, pp. 775–784.
[19] Wen, D. Ding, Y. Formulation of nanofluids for natural convective heat transfer applications, *Int. J. Heat and Fluid Flow*, 26, 2005, pp. 855–864.
[20] Wen, D. Ding, Y. Natural convection heat transfer of suspensions of titanium dioxide nanoparticles (nanofluids), *IEEE Trans. Nanotechnol.*, 5(3), 2006, pp. 220–227.
[21] Li, C.H. Peterson, G.P. Experimental studies of natural convection heat transfer of Al2O3/DI water nanoparticle suspensions (nanofluids), *Advances in Mechanical Engineering*, 2010, Article ID 742739.
[22] Hu, Y., He, Y., Wang, S., Wang, Q. Schlaberg, H.I. Experimental and numerical investigation on natural convection heat transfer of Tio2–Water nanofluids in a square enclosure, *ASME Journal of Heat Transfer*, 136, 2014, Article ID 022502.
[23] Nnanna, A.G.A. Experimental model of temperature-driven nanofluid, *ASME Journal of Heat Transfer*, 129, 2007, pp.697–704.
[24] Ho, C.J., Liu, W.K., Chang, Y.S. Lin, C.C. Natural convection heat transfer of alumina-water nanofluid in vertical square enclosures: An experimental study, *Int. J. Thermal Sciences*, 49, 2010, pp.1345–1353.
[25] Corcione, M. Heat transfer features of buoyancy-driven nanofluids inside rectangular enclosures differentially heated at the sidewalls, *Int. J. Thermal Sciences*, 49, 2010, pp.1536–1546.
[26] Kestin, J., Sokolov, M. Wakeham, W.A. Viscosity of liquid water in the range -8 °C to 150 °C., *J. Phys. Ref. Data*, 7(3), 1978, pp. 941–948.
[27] Sharqawy, M.H. New correlations for seawater and pure water thermal conductivity at different temperatures and salinities, *Desalination*, 313, 2013, pp. 97–104.
[28] Patankar, S.V. *Numerical Heat Transfer and Fluid Flow*, Hemisphere Publishing Corporation, Taylor and Francis Group, New York, 1980.
[29] Versteeg, H.K. Malalasekera, W. *An Introduction to Computational Fluid Dynamic: The Finite Volume Method*, John Wiley Sons Inc., New York, 1995.
[30] Fusegi, T. Hyun, J.M. Laminar, Transitional natural convection in an enclosure with complex, realistic conditions, *Int. J. Heat Fluid Flow*, 15, 1994, pp. 258–268.
[31] Abu-Nada, E. Effects of variable viscosity and thermal conductivity of Al2o3–water nanofluid on heat transfer enhancement in natural convection, *Int. J. Heat and Fluid Flow*, 30, 2009, pp. 679–690.
[32] Abu-Nada, E. Chamkha, A.J. Effect of nanofluid variable properties on natural convection in enclosures filled with a CuO-EG-Water nanofluid, *Int. J. Thermal Sciences*, 49, 2010, pp. 2339–2352.